AD-A133 907 VERY LARGE ARRAY OBSERVATIONS OF SOLAR ACTIVE REGIONS 1/1
IV STRUCTURE AND EV..(U) TUFTS UNIV MEDFORD MA DEPT OF
PHYSICS R F WILLSON ET AL. JUL 83 AFOSR-TR-83-0843
UNCLASSIFIED AFOSR-83-0019 F/G 3/2 NL

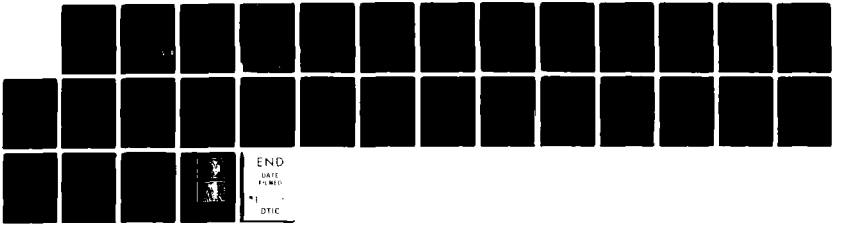

END
DATE FILMED
DTIC

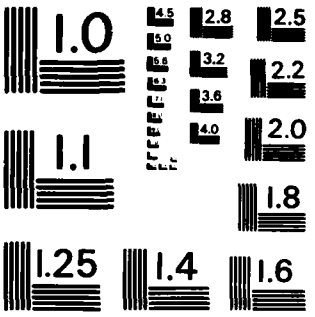

MICROCOPY RESOLUTION TEST CHART
NATIONAL BUREAU OF STANDARDS - 1963 - A

VERY LARGE ARRAY OBSERVATIONS OF SOLAR ACTIVE REGIONS

IV. STRUCTURE AND EVOLUTION OF RADIO BURSTS FROM 20 CM LOOPS

Robert F. Willson and Kenneth R. Lang

Department of Physics

Tufts University

To appear in the Astrophysical Journal

SECURITY CLASSIFICATION OF THIS PAGE (When Data Entered)

REPORT DOCUMENTATION PAGE

READ INSTRUCTIONS BEFORE COMPLETING FORM

1. REPORT NUMBER: AFOSR-TR- 83-0843	2. GOVT ACCESSION NO.: AD-A133907
3. RECIPIENT'S CATALOG NUMBER:	
4. TITLE (and Subtitle): VERY LARGE ARRAY OBSERVATIONS OF SOLAR ACTIVE REGIONS IV. STRUCTURE AND EVOLUTION OF RADIO BURSTS FROM 20 CM LOOPS	5. TYPE OF REPORT & PERIOD COVERED: Interim
	6. PERFORMING ORG. REPORT NUMBER:
7. AUTHOR(s): Robert F. Willson and Kenneth R. Lang	8. CONTRACT OR GRANT NUMBER(s): AFOSR-83-0019
9. PERFORMING ORGANIZATION NAME AND ADDRESS: Tufts University Department of Physics Medford, MA 02155	10. PROGRAM ELEMENT, PROJECT, TASK AREA & WORK UNIT NUMBERS: 61102F [redacted] 2311/A1
11. CONTROLLING OFFICE NAME AND ADDRESS: AFOSR /NP Bolling AFB, Bldg. #410 Washington, DC 20332	12. REPORT DATE: July 1983
	13. NUMBER OF PAGES: 28
14. MONITORING AGENCY NAME & ADDRESS(if different from Controlling Office):	15. SECURITY CLASS. (of this report): Unclassified
	15a. DECLASSIFICATION/DOWNGRADING SCHEDULE:

16. DISTRIBUTION STATEMENT (of this Report)

Approved for public release; distribution unlimited

17. DISTRIBUTION STATEMENT (of the abstract entered in Block 20, if different from Report)

18. SUPPLEMENTARY NOTES

To appear in Astrophysical Journal

19. KEY WORDS (Continue on reverse side if necessary and identify by block number)

Sun: radio radiation - Sun: radio bursts - Sun: magnetic fields - Sun: activity

20. ABSTRACT (Continue on reverse side if necessary and identify by block number)

The Very Large Array (VLA) has been used to study the structure and evolution of six solar bursts near 20 cm wavelength. In most cases the burst emission has been resolved into looplike structures with total lengths, $L \sim 3 \times 10^9$ cm, brightness temperatures $T_B \sim 10^7$ to 10^8 K and degrees of circular polarization $\rho_c \lesssim 90\%$. Changes in the total intensity and circular polarization of the bursts occur on timescales as short as ten seconds.

DD FORM 1 JAN 73 1473

unlimited

SECURITY CLASSIFICATION OF THIS PAGE (When Data Entered)

The individual peaks of one multiple component burst originated in different locations within a magnetically complicated region. Preburst heating and circular polarization changes respectively occurred minutes before the onset of the impulsive phase of two bursts. In one case a loop system emerged in the vicinity of the impulsive source, and two adjacent loop systems may have emerged and triggered the burst.

ABSTRACT

The Very Large Array (VLA) has been used to study the structure and evolution of six solar bursts near 20 cm wavelength. In most cases the burst emission has been resolved into looplike structures with total lengths, $L \sim 3 \times 10^9$ cm, brightness temperatures $T_B \sim 10^7$ to 10^8 K and degrees of circular polarization, $\rho_c \lesssim 90\%$. Changes in the total intensity and circular polarization of the bursts occur on timescales as short as ten seconds. The individual peaks of one multiple component burst originated in different locations within a magnetically complicated region. Preburst heating and circular polarization changes respectively occurred minutes before the onset of the impulsive phase of two bursts. In one case a loop system emerged in the vicinity of the impulsive source, and two adjacent loop systems may have emerged and triggered the burst.

Subject headings: interferometry - polarization - Sun: activity - Sun: bursts - Sun: coronal loops - Sun: magnetic fields - Sun: radio radiation

A

I. INTRODUCTION

Centimeter wavelength (λ = 2 cm or 6 cm) observations with the Very Large Array (VLA) at high angular resolution $\theta \geq 1''$ and moderate time resolution $\tau \approx 10$ s have provided new insights into the physics of solar radio bursts. The radio bursts are usually located above magnetic neutral lines rather than sunspots, while the Hα flares often occur near the sunspots (Marsh et al. 1979; Marsh and Hurford 1980; Lang, Willson and Felli 1981; Willson 1983). The total intensity and circular polarization of the radio emission often change before the bursts, suggesting that they are triggered by preburst heating or by magnetic changes. Variations in the distribution of circular polarization also reflect changes in the magnetic field configuration during solar bursts (Kundu, Bobrowsky and Velusamy 1982; Velusamy and Kundu 1982; Willson 1983). The observations at λ = 2 cm and 6 cm therefore suggest that radio bursts are emitted near the apex of magnetic loops, rather than at their feet; and that either preburst heating within loops or emerging loops trigger burst emission.

There have been comparatively few VLA observations of solar bursts at the longer 20 cm wavelength. Observations of the quiescent emission from solar active regions at λ = 20 cm delineate looplike structures which are the radio wavelength counterpart of the ubiquitous coronal loops detected at soft X-ray wavelengths (Lang, Willson and Rayrole 1982). Velusamy and Kundu (1981) have reported the detection of a post-flare loop at λ = 20 cm, and Lang, Willson and Felli (1981) have shown that some 20 cm bursts have small angular sizes $\theta \sim 3''$ to $5''$ and brightness temperatures $T_B \sim 2 \times 10^7$ K that are respectively similar to those of hard X-ray kernels and soft X-ray bursts. The 20 cm data are nevertheless meager, and in this paper we therefore

present a VLA analysis of six bursts from 20 cm loops. In §II we present time profiles and 10 s snapshot maps that describe the evolution of the 20 cm bursts, preburst heating, and changes in magnetic structure before and during the bursts. The angular sizes $\theta \sim 20"$ to $60"$, total linear extents $L \sim 0.7$ to 5×10^9 cm and brightness temperatures $T_B \sim 2$ to 20×10^7 K of the 20 cm bursts are similar to those observed at soft X-ray wavelengths. In §III we discuss the implications of our observations, and place them within the framework of other observational and theoretical work.

II. OBSERVATIONS OF RADIO BURSTS FROM 20 CM LOOPS

The Very Large Array (B configuration) was used to observe the active region AR 3804 on 1982 July 12 to 20 at 1380 MHz, 1540 MHz or 1705 MHz (or wavelengths λ = 21.7, 19.4 and 17.6 cm). On July 12 the active region was observed for successive 10 minute periods at 1380 MHz and 1705 MHz, while on July 19 and 20 the region was observed at all three frequencies for successive 10 minute intervals. At these frequencies the half-power beamwidth of the individual antenna is $\sim 31'$ and the synthesized beamwidth was $3" \times 4"$. Each 10 minute observation was followed by a 2 minute observation of the calibrator source OI 318. In all cases the bandwidth was 12.5 MHz and the assumed calibrator flux was 1.7 Jy. The average correlated flux of 356 interferometer pairs was sampled every 10 s for both the left hand circularly polarized (LCP) and right hand circularly polarized (RCP) signals. The amplitude and phase of the correlated signal were then calibrated according to the procedure described by Lang and Willson (1979) together with a correction for the difference in the signal from high temperature noise sources detected in each polarization

channel. These data were then edited and used to produce synthesis maps of both the total intensity, I = (RCP+LCP)/2 and circular polarization V = (RCP-LCP)/2 of the burst emission at intervals of 10 s. The CLEAN procedure developed by Clark (1980) was then used to produce synthesis maps with a dynamic range of about 10:1.

The date, time, observing wavelength, maximum brightness temperature and maximum degree of circular polarization, and angular size for six bursts are given in Table I. In Figure 1 we show the time profile of the spikelike burst on July 12. The rapid impulsive spike lasting $\sim$60 s is superimposed on a more gradual component lasting about 2 m. In Figure 2 we present 10 s snapshot maps of both the total intensity, I, and circular polarization, V, for both of these components. The impulsive spike consists of two components of unequal intensity and size that are separated by about 45" and which are nearly 100% oppositely circularly polarized. These two components are also connected by a bridge of weaker, unpolarized emission. The gradual component, which began about 1 m before the impulsive spike, is contained within an adjacent source having a peak brightness temperature of $T_B \sim 6 \times 10^6$ K and a polarization of about 100%, suggesting that preburst heating in an adjacent part of the active region triggered the impulsive spike. The impulsive emission occurred mainly along the legs of a magnetic loop. Kundu and Vlahos (1979) have shown that if the magnetic field strengths at the feet of a loop are different or if unequal numbers of particles are injected downward along each leg, then both the intensity and degree of circular polarization of the two microwave sources will be different, as is the case here. The bipolar structure of this burst is nevertheless uncommon, for the impulsive component of most microwave bursts occurs at the apex of coronal loops, rather than along their legs.

Figure 3 shows the time profile of a multiple-spike burst on July 12. The fourth and fifth spikes were associated with an Hα flare. Snapshot maps coinciding with the peaks of the spikes (Figure 4) show that the most intense peaks (1, 4 and 5 in Figure 3) arise from spatially separated structures having peak brightness temperatures between 2×10^7 K and 1.5×10^8 K and angular extents between 20" and 50" (linear extents $L = 1.4$ to 3.5×10^9 cm). The weaker spikes (2, 3 and 6 in Figure 3) that followed a more intense spike were, however, located in the same source as the intense one. Thus, successive weak spikes seem to be emitted in the same loop, while successive intense spikes are emitted from different loops. This last conjecture is supported by the circular polarization changes that reflect different magnetic structures at the times of successive intense spikes.

In Figure 5 we show VLA synthesis maps of the preburst emission made during a 15 minute interval before the start of the first impulsive spike shown in Figure 3. Each map was made from 2 minutes of data beginning at the time indicated. Here the dashed boxes refer to the field of view of the 10 s snapshot maps of the impulsive spikes shown in Figure 4. Both the total intensity and circular polarization increased and changed in an adjacent source during the 15 m preceding the first spike. At 18:51:55 UT the peak brightness temperature of this adjacent source was $T_B \sim 7 \times 10^6$ K, about a factor of 3 to 4 above the brightness temperature typically observed in coronal radio loop structures (Kundu et al. 1978; Felli, Lang and Willson 1981; Lang, Willson and Rayrole 1982). The adjacent source began to heat up about 30 m before the onset of the impulsive spikes, and remained at $T_B \sim 7 \times 10^6$ K until 5 m before the first impulsive spike. At this time the region of spiked emission began to heat up, while the adjacent

source cooled to $T_B \sim 4 \times 10^6$ K. This newly heated region of spiked emission was about 60% right circularly polarized, suggesting that it occurred in one leg of a coronal loop.

In Figure 6 we show the time profile of the July 19 burst whose evolution is shown in Figure 7. This event consists of two components, whose combined duration was 70 s. The burst structure at first consisted of two sources separated by a bridge of weaker emission. The polarization maps, which are not shown here, indicated that these two sources were oppositely circularly polarized ($\rho_c \sim 20$-30%) and that they therefore probably mark the legs of magnetic loops. The more intense source disappeared in 10 s as the weaker source became larger. In an additional 10 s, the initially more intense source brightened again, as the initially weaker source faded away. Craig and McClymont (1976) and Antiochos and Sturrock (1982) have pointed out that mass motions may play a role in the cooling of flare loops. Because a flare loop is known to be cooler at the base than at the top, pressure gradients will develop which in turn generate large down flows of coronal material. One interpretation of the burst structure shown in Figure 7 is that during the two peaks of most intense emission the loop was filled by hot plasma which then flowed down alternate legs, suggesting cooling by mass motions. The preburst maps of this burst showed no detectable temperature enhancements or changes in circular polarization on timescales of minutes to several hours before the beginning of the burst.

In Figure 8 we show the time-profile of the July 20 burst, whose evolution is shown in Figure 9. A looplike structure having a peak brightness temperature of $\sim 5 \times 10^6$ K corresponds to the weak precursor, shown in Figure 8. Rapid polarization changes occurred before the main burst, with the emergence of A and B at 23:10:10 UT and the disappearance of B and C at 23:10:20 UT

(see Figure 9). The circularly polarized emission may correspond to the feet of two dipolar loop systems A-B and C-D which respectively emerged at 23:10:10 and 23:09:40 UT. The impulsive spike occurring at 23:10:40 UT is contained within a looplike structure, but it is oriented perpendicular to the preburst loop. The impulsive peak is also located nearly between the oppositely polarized sources A and B, and may have been triggered by the emergence of this loop. The impulsive source apparently moved by $\sim$ 10" to the west during this time interval. This limbward displacement could be explained as an outward motion of the burst source or as the brightening of progressively higher-lying loops. If the burst is moving radially outward from the surface of the Sun, then the inferred velocity is $\sim$ 370 km s^{-1}. For comparison, the velocities of moving type IV bursts typically range between 250 and 1200 km s^{-1} (Pick and Trotter 1978; Robinson 1978; Kai 1978) while outward motions of 250 to 400 km s^{-1} have been detected in coronal X-ray burst loops (Poland et al. 1982; Antonucci et al. 1982).

In Figure 10 we compare the impulsive phase of this burst as well as that of another burst which began on the same day with simultaneous Hα photographs showing the underlying optical flares. Here the uncertainty in the alignment between the radio and optical pictures is ±5". The figure shows that the centroids of both radio images are displaced limbwards by $\sim$ 30" to 40" with respect to the Hα kernels. This displacement can be attributed as a radial, limbward displacement caused by the greater height of the 20 cm emission, indicating a height h = (2 to 3±0.4) x 10^9 cm above the solar photosphere. These values are consistent with the height h $\sim$ 3 to 4 x 10^9 cm for quiescent loops (Lang, Willson and Gaizauskas 1983).

III. DISCUSSION

The observations presented here provide new insight into the evolution of solar microwave bursts and the physical processes which may trigger them. In one case, the intense components of multiple bursts originated in different sources, suggesting that a number of loops may have become successively activated like some complex X-ray bursts (Vorpahl et al. 1975; Kahler, Krieger and Vaiana 1975). There is evidence for different magnetic field strengths at different times in the evolution of these X-ray bursts (Karpen et al 1979). Because only a few percent of the magnetic energy is expected to be converted to particle energy during the impulsive phase (Baum and Bratenahl 1976) both the radio and X-ray results suggest that the components of intense multiple bursts originate in separate locations within an active region. On the other hand, this does not always occur for Kundu, Bobrowsky and Velusamy (1982) and Lang, Willson and Felli (1981) found that the positions of the individual peaks of multiple component microwave bursts were at the same location to within a few seconds of arc, and we also found that weaker successive components originate in the same source.

We also found evidence for both preburst heating and magnetic changes that may have triggered the impulsive energy release in the loops. (Also see Lang, 1974; Syrovotskii and Kuznetzov 1980; Syrovotskii and Somov 1980; Webb and Kundu 1978; Webb 1980). The cause of the sudden temperature enhancements is uncertain. It is possible that we are viewing portions of magnetic loops where the opacity due to either gyroemission or thermal bremsstrahlung increased, thereby causing a temperature increase. Kundu et al (1982) have speculated that if the dominant radiation mechanisms in preflare coronal loops is gyroemission, then the onset of currents in the loop could increase the magnetic field strength to make the source optically thick at the third

harmonic of the gyrofrequency (170 gauss at 20 cm). It is interesting to note, however, that for the burst which began at 19:04 UT on July 12, the impulsive sources were both left and right circularly polarized, whereas the newly heated preburst source was only right circularly polarized, suggesting that the impulsive and preburst sources were located in a different set of loops. In another case we found that a loop system emerged about 20 seconds before the impulsive phase of the burst. Recently Kundu et al. (1982) observed a similar polarization change only a few tens of seconds before a 6 cm burst, which they believe to be related to the impulsive energy release. The quadrupole field configuration observed in these cases evokes flare models in which neighboring loops merge together and form current sheets between the interface of the loops, thereby triggering the impulsive phase of the burst (Gold and Hoyle 1960; Heyvaerts et al. 1977; Emslie 1982).

There were also cases where preburst changes were undetectable on timescales of minutes to several hours before the onset of the impulsive phase. Out of eight bursts observed at 2, 6 and 20 cm by Willson (1983) only one exhibited detectable preburst heating of the coronal loop in which the burst took place. These results suggest that preburst changes in the centimeter wavelength emission of coronal loops are not a general feature of the burst process, at least for relatively small bursts of a few solar flux units in size. A similar conclusion was reached by Kahler (1979) and Mosher and Acton (1980) who found no compelling evidence for X-ray enhancements during the few tens of minutes before weak X-ray events.

Solar radio astronomy at Tufts University is supported under grant AFOSR-83-0019 with the Air Force Office of Scientific Research. We are

grateful to Margaret Liggett of the Big Bear Solar Observatory for providing the Hα photographs. The Very Large Array is operated by Associated Universities Inc., under contract with the National Science Foundation.

REFERENCES

Antiochos, S.K. and Sturrock, P.A. 1982, Solar Phys. 254, 343.

Antonucci, E., Gabriel, A.H., Acton, L.W., Culhane, J.L., Doyle, J.G., Liebacher, J.W., Machado, M.E., Orwig, L.E. and Rapley, C.G. 1982, Solar Phys. 78, 107.

Baum, P.J. and Bratenahl, A. 1976, Solar Phys. 47, 331.

Clark, B.G. 1980, Astron. Astrophys. 89, 377.

Craig, I.J.D. and McClymont, A.N. 1976, Solar Phys. 50, 133.

Emslie, A.G. 1982, Astrophys. Lett. 22, 41.

Felli, M., Lang, K.R. and Willson, R.F. 1981, Ap. J., 247, 325.

Gold, T. and Hoyle, F. 1960, MNRAS, 85, 553.

Heyvaerts, J., Priest, E.R. and Rust, D.M. 1977, Ap. J. 216, 123.

Kahler, S.W. 1979, Solar Phys. 62, 347.

Kahler, W.S., Krieger, A.S. and Vaiana, G.S. 1975, Ap. J. (Letters) 199, L57.

Kai, K. 1978, Solar Phys. 61, 187.

Karpen, J.T., Crannel, C.J. and Frost, K.J. 1979, Ap. J. 234, 370.

Kundu, M.R., Alissandrakis, C.E., Bregman, J.D. and Hin, A.C. 1978, Ap. J. 213, 278.

Kundu, M. and Vlahos, L. 1979, Ap. J., 232, 595.

Kundu, M.R., Bobrowsky, M. and Velusamy, T. 1982, Ap. J. 251, 342.

Kundu, M.R., Schmahl, E.J., Velusamy T. and Vlahos, T. 1982, Astron. Astrophys. 108, 188.

Lang, K.R. 1974, Solar Phys. 36, 351.

Lang, K.R. and Willson, R.F. 1979, Nature 278, 24.

Lang, K.R., Willson, R.F. and Felli, M. 1981, Ap. J. 247, 338.

Lang, K.R., Willson, R.F. and Rayrole, J. 1982, Ap. J. 258, 284.

Lang, K.R., Willson, R.F. and Gaizauskas, V. 1983, Ap. J., 267, 455.

Marsh, K.A., Zirin, H. and Hurford, G.J. 1979, Ap. J. 228, 610.

Marsh, K.A. and Hurford, G.J. 1980, Ap. J. (Letters) 240, L111.

Mosher, J. and Acton, L. 1980, Solar Phys. 66, 105.

Pick, M. and Trotter, G. 1978, Solar Phys. 60, 353.

Poland, A.I., Machado, M.E., Wolfson, Frost, K.J., Woodgate, B.E., Shine, R.A., Kenny, P.J., Cheng, C.C., Tandberg-Hanssen, E., Bruner, E.C., and Henze, W. 1982, Solar Phys. 78, 201.

Robinson, R.D. 1978, Solar Phys. 60, 383.

Syrovotskii, S.I. and Kuznetzov, V.D. 1980, Radio Physics of the Sun, eds. M.R. Kundu and T.E. Gergeley (Dordrecht: Reidel), P.445.

Syrovotskii, S.I. and Somov, B.V. 1980, in IAU Symposium 91, Solar and Interplanetary Dynamics, eds. M. Dryer and E. Tandberg-Hanssen (Dordrecht: Reidel), p.425.

Velusamy, T. and Kundu, M.R. 1981, Ap. J. (Letters), 243, L103.

Velusamy, T. and Kundu, M.R. 1982, Ap. J. 258, 388.

Vorpahl, J.A., Gibson, E.G., Landecker, P.B., McKenzie, D.L. and Underwood, J.H. 1975, Solar Phys. 45, 199.

Webb, D.F. and Kundu, M.R. 1978, Solar Phys. 57, 155.

Webb, D.F. 1980, in IAU Symposium 91, Solar and Interplanetary Dynamics eds. M. Dryer and E. Tandberg-Hanssen (Dordrecht: Reidel).

Willson, R.F. 1983, Solar Phys. (in press).

KENNETH R. LANG and ROBERT F. WILLSON:

Department of Physics, Tufts University

Medford, MA 02155, U.S.A.

TABLE 1

Observed Parameters of Solar Bursts near 20 cm Wavelength.

Date	Time (UT)	Wavelength (cm)	Maximum Brightness Temperature (K)	Maximum Circular Polarization (percent)	Angular Size (")
7/12/82	15:31-15:32	21.7	1.5×10^8	$\sim$ 90	$\sim$ 45
7/12/82	19:05-19:09	17.6	1.4×10^8	$\sim$ 70	$\sim$ 30
7/12/82	20:03-20:07	21.7	2.0×10^7	$\sim$ 20	$\sim$ 40
7/19/82	18:41-18:43	19.4	1.2×10^7	$\sim$ 40	$\sim$ 60
7/20/82	21:49-21:51	19.4	1.3×10^7	$\sim$ 60	$\sim$ 60
7/20/82	23:10-23.12	17.6	4.9×10^7	$\sim$ 25	$\sim$ 45

Figure Legends

Fig. 1. The fringe amplitude and total intensity, I, versus time for a spikelike burst detected at 20 cm wavelength with an interferometer pair with angular resolution θ = 45" on July 12, 1982.

Fig. 2. A series of 10 s snapshot maps of the total intensity, I, and circular polarization, V, for the burst shown in Figure 1. The contours of the map mark levels of equal brightness temperature, and the solid and dashed contours of the V maps denote positive and negative values of V, respectively. The development of the gradual burst emission is shown on the left hand side. Maps of the impulsive phase are shown on the right hand side. The outermost contour level and the contour interval of the gradual component maps are 2.4×10^6 K and 1.2×10^6 K, respectively. The outermost contour and contour interval of the impulsive phase maps are both equal to 7.2×10^6 K. The angular scale can be determined from the 30" spacing between the fiducial marks on the axes.

Fig. 3. The time profile of a multiple-spike burst detected at 20 cm wavelength with an interferometer pair with angular resolution θ = 45" on July 12, 1982.

Fig. 4. A series of 10 s snapshot maps made at the most intense peaks (1, 4 and 5) of the impulsive spikes of the complex burst whose time profile is shown in Figure 3. The contours of the maps mark levels of equal brightness temperature and the solid and dashed contours of the V maps denote positive and negative values of V, respectively. For both sets of maps the outermost contour and the contour interval are both equal

to 1.0 x 10^7 K. The angular scale can be determined from the 30" spacing between the fiducial marks on the axes.

Fig. 5. A series of VLA maps showing the development of the active region AR 3804 before the complex burst shown in Figure 3. Each map of total intensity, I (top), and circular polarization, V (bottom), was made from 2 m of data beginning at the time indicated. The contour of both sets of maps mark levels of equal brightness temperature and the solid and dashed lines of the V maps denote positive and negative values of V, respectively. For both sets of maps the outermost contour level and the contour interval are equal to 1.7 x 10^6 K. The angular scale can be determined from the 60" spacing between the fiducial marks on the axes. The area within the dashed boxes corresponds to the field of view of the 10 s snapshot maps which are shown in Figure 4.

Fig. 6. The fringe amplitude of the total intensity, I, versus time for a burst detected at 20 cm wavelength with an interferometer pair with an angular resolution θ = 35" on July 19, 1982.

Fig. 7. A series of 10 s snapshot maps of the total intensity, I, for the burst shown in Figure 6. The outermost contour and the contour interval are both equal to 1.3 x 10^6 K. The angular scale is determined by the 30" spacing between the fiducial marks on the axes.

Fig. 8. The fringe amplitude, I, versus time for a burst detected at 20 cm wavelength with an interferometer pair whose angular resolution θ = 45" on July 20, 1982.

Fig. 9. A series of 10 s VLA snapshot maps of the total intensity, I, and circular polarization, V, for the burst shown in Figure 8. The development of the pre-burst emission is shown on the left hand side. Maps of the

impulsive phase are shown on the right hand side. The outermost contour level and the contour interval of the preburst emission are both equal to 1.7×10^6 K. The outermost contour and contour level of the impulsive phase are both equal to 8.2×10^6 K. The curved line in the upper right hand side of each box denotes the solar west limit. The angular scale can be inferred from the 30" spacing between fiducial marks on the axes.

Fig. 10. A 10 s VLA synthesis map of the impulsive phase of two bursts detected at 20 cm wavelength on July 20, 1982. The radio maps have been superimposed on an Hα photograph of the optical flares taken at the same time. For both images, north is up, west is to the right. The Hα photograph was taken at the Big Bear Solar Observatory (courtesy of Margaret Liggett).

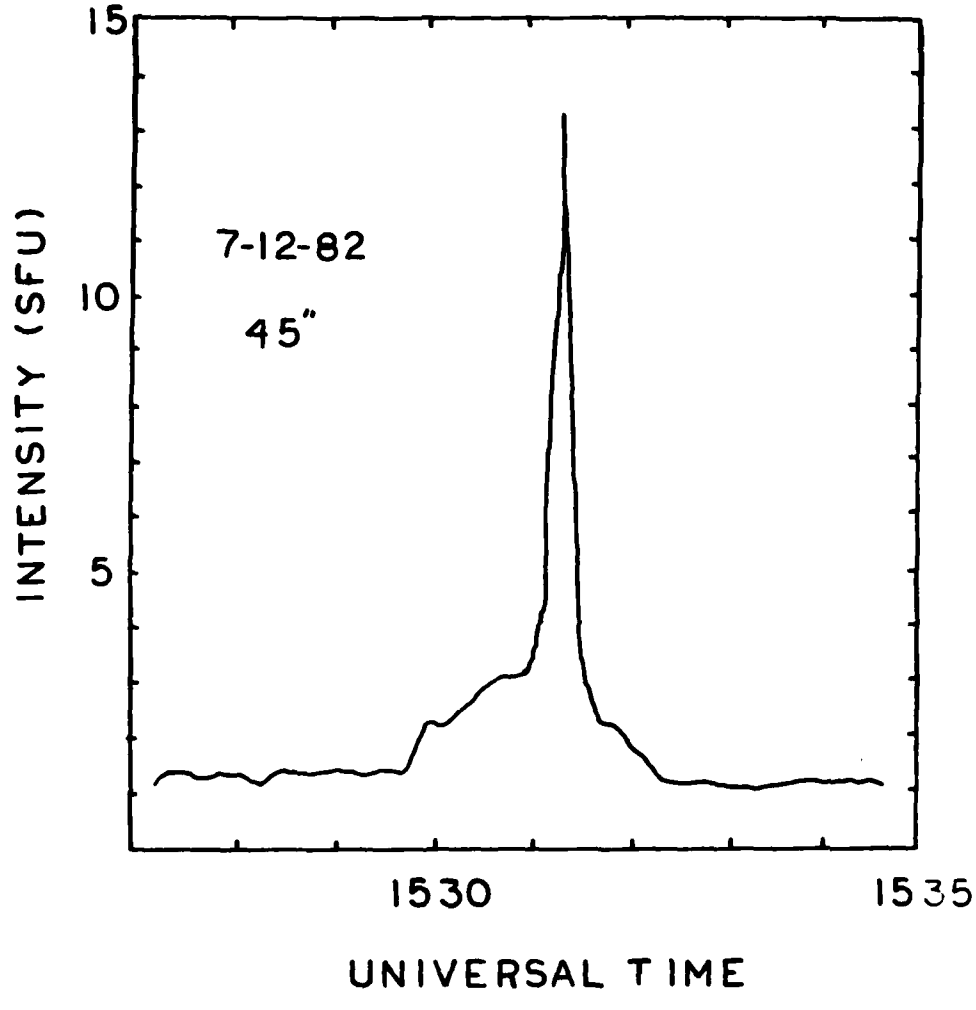
15
10
5
INTENSITY (SFU)
7-12-82
45"
1530
1535
UNIVERSAL TIME

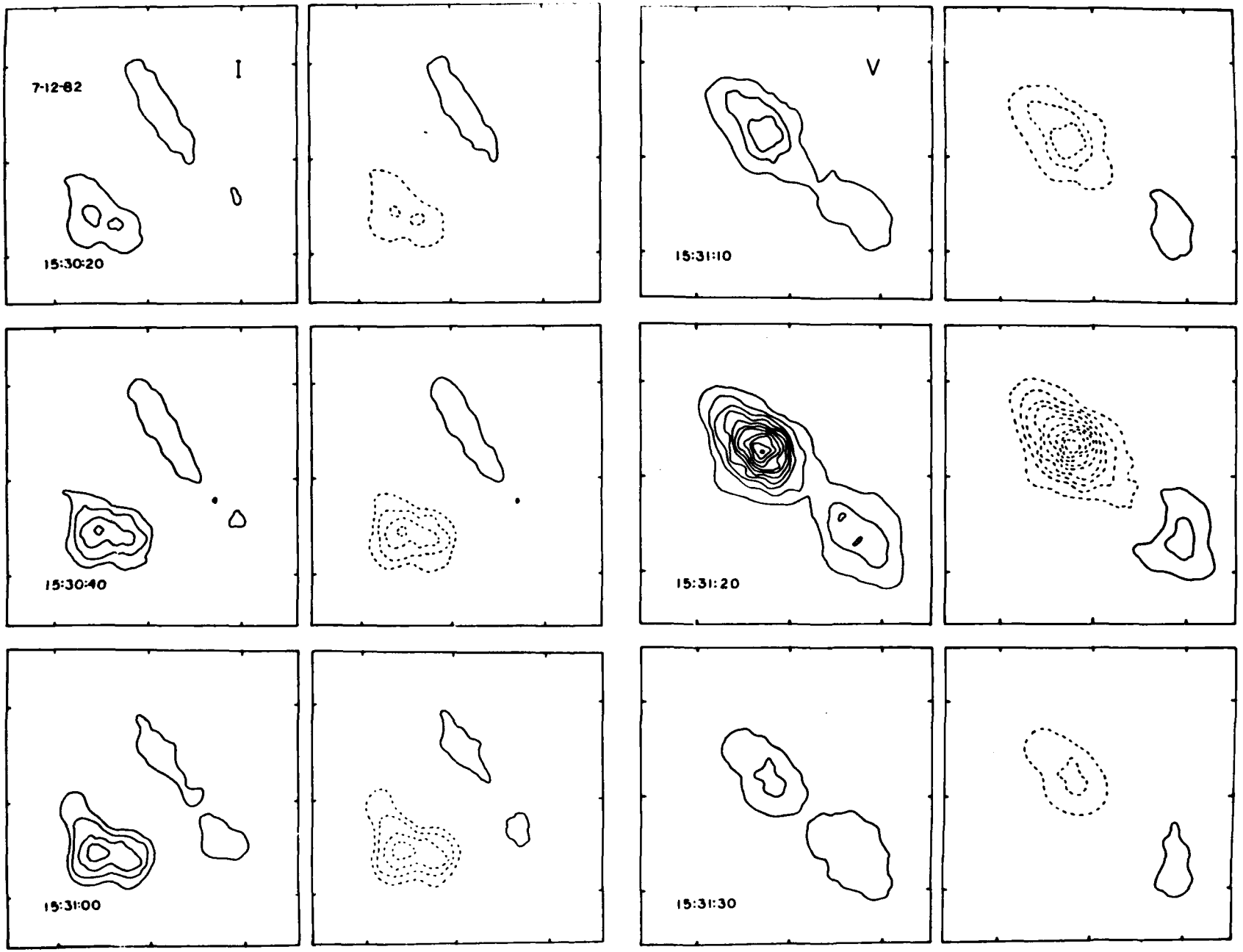
7-12-82
I
15:30:20
V
15:31:10
15:30:40
15:31:20
15:31:00
15:31:30

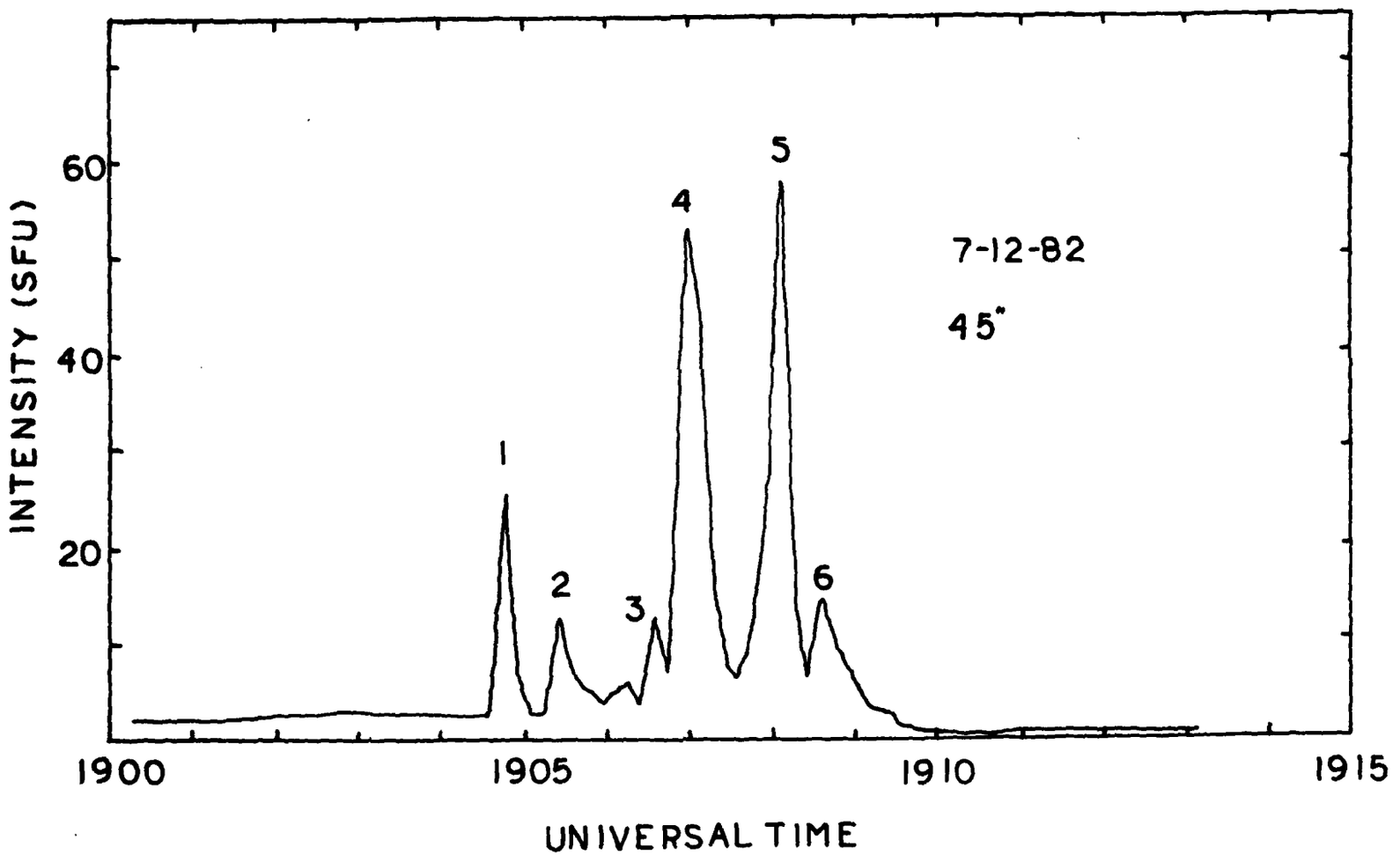
INTENSITY (SFU)
60
40
20
1
2
3
4
5
6
7-12-82
45°
1900
1905
1910
1915
UNIVERSAL TIME

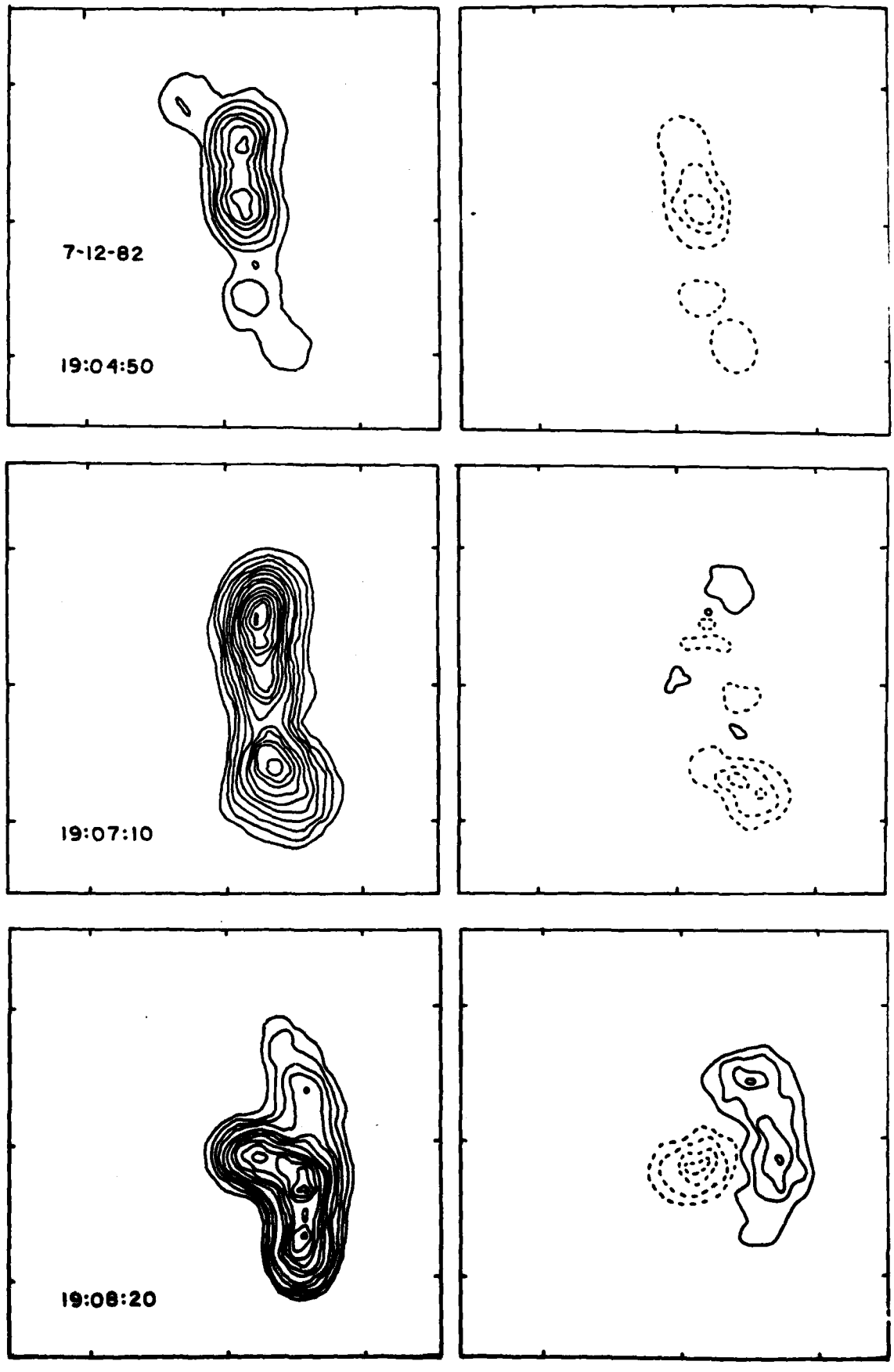
7-12-82
19:04:50
19:07:10
19:08:20

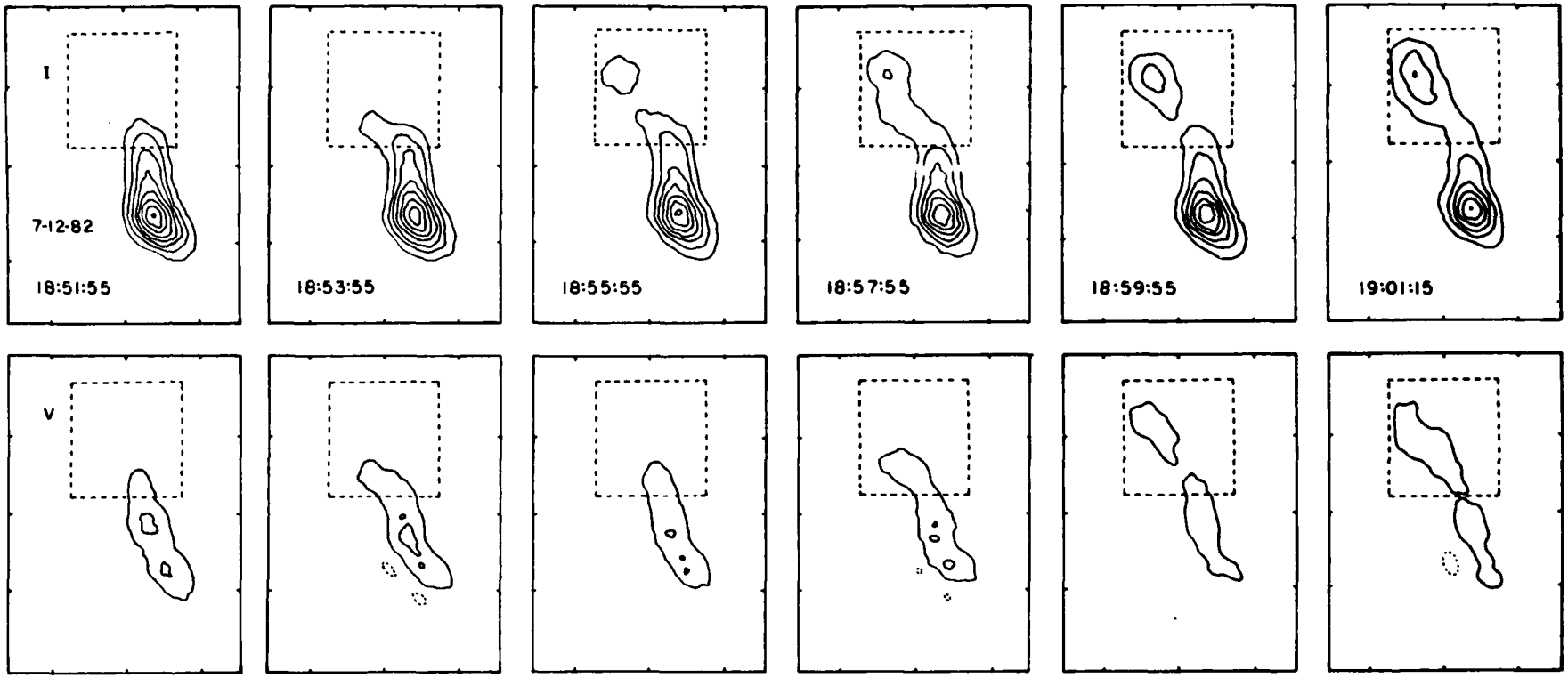
I
7-12-82
18:51:55
18:53:55
18:55:55
18:57:55
18:59:55
19:01:15
V

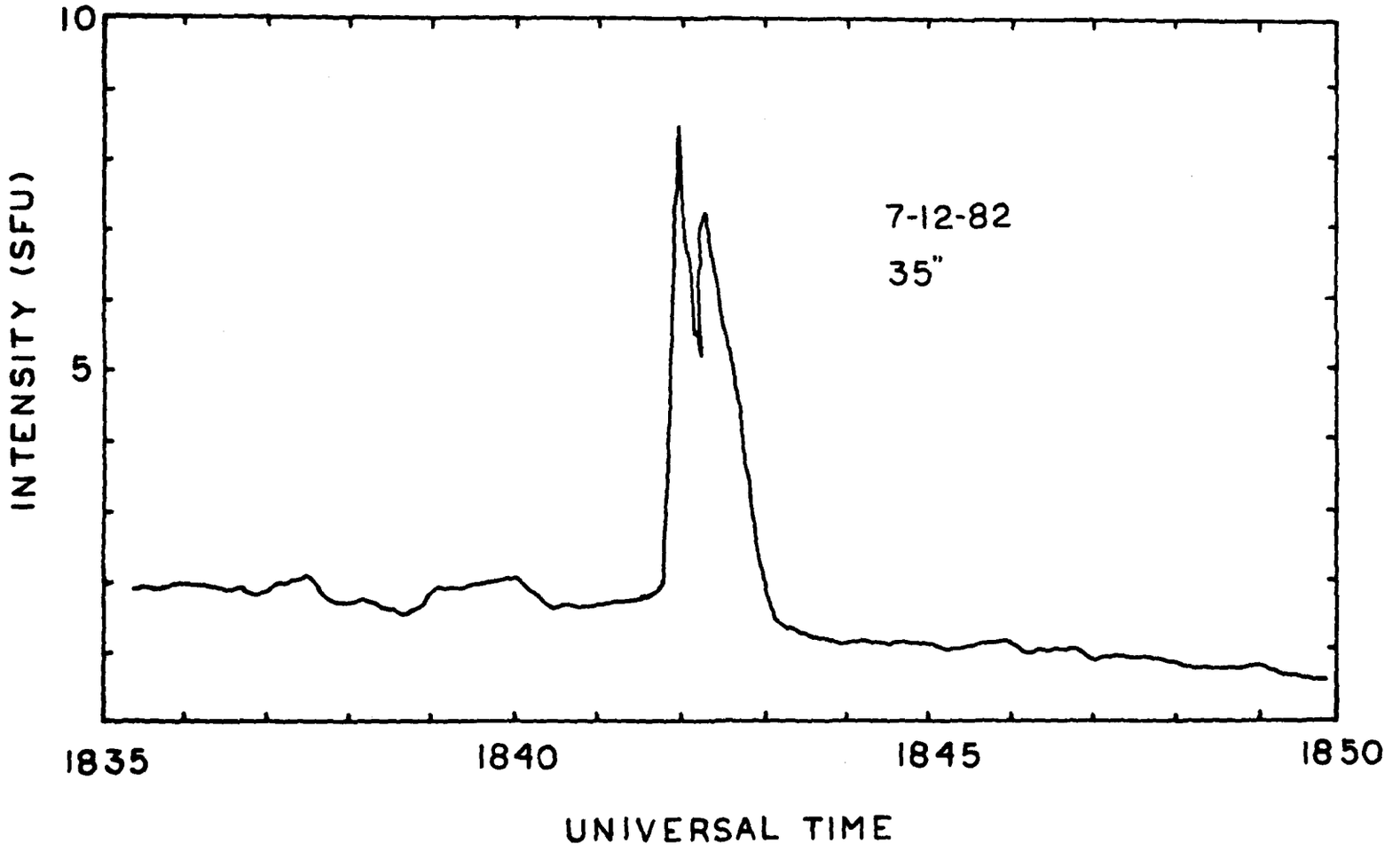
10
5
INTENSITY (SFU)
7-12-82
35"
1835
1840
1845
1850
UNIVERSAL TIME

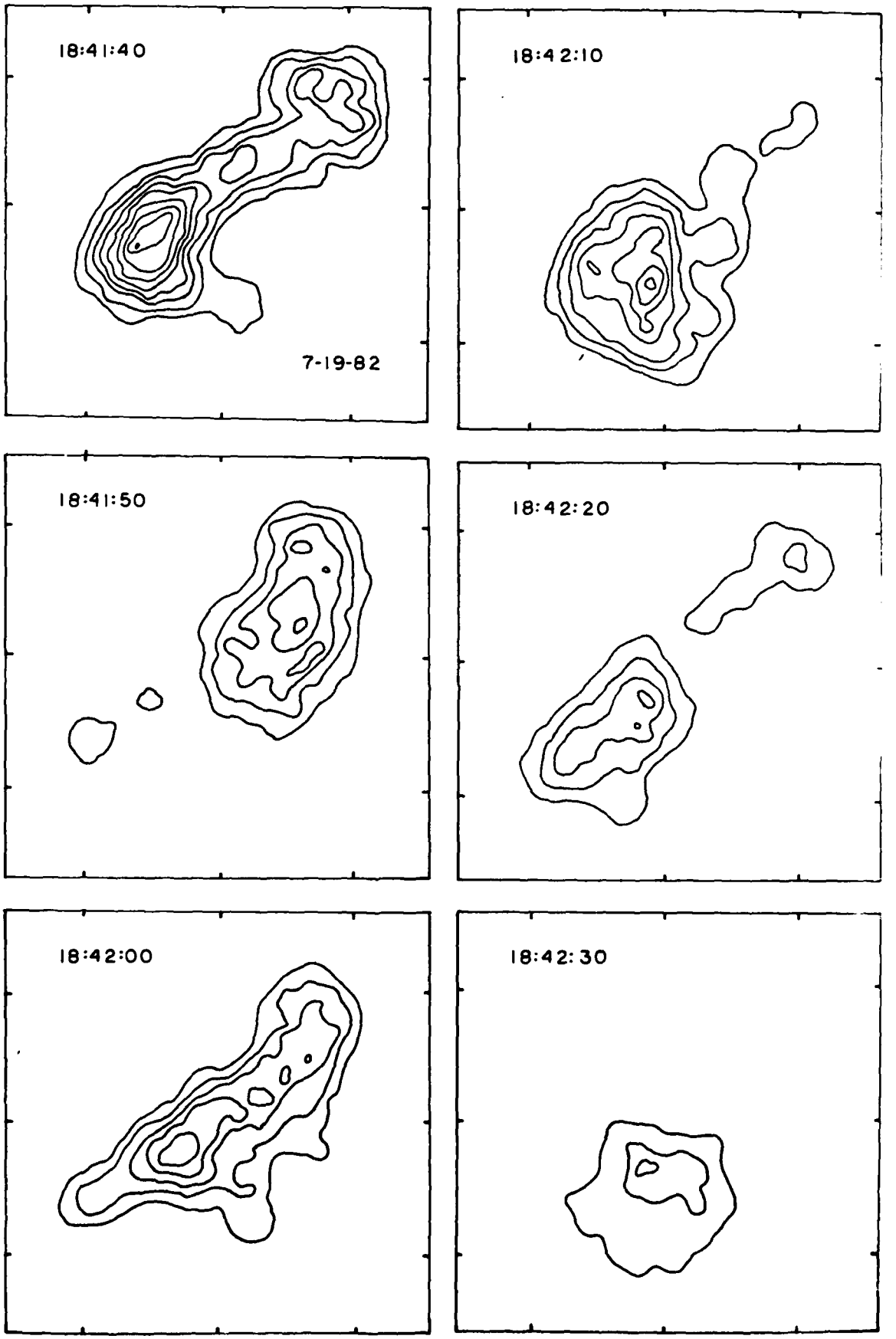
18:41:40
7-19-82
18:42:10
18:41:50
18:42:20
18:42:00
18:42:30

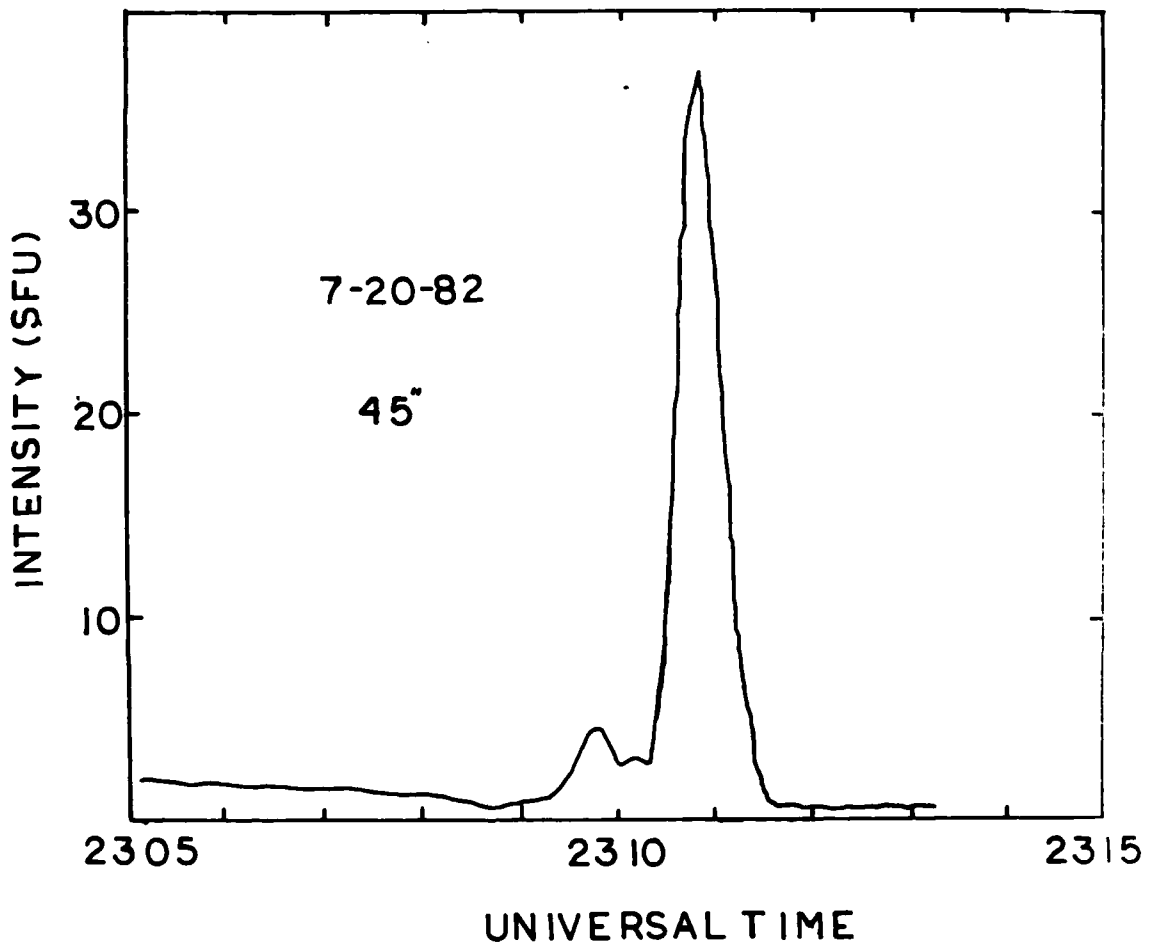
INTENSITY (SFU)
30
20
10
7-20-82
45°
2305
2310
2315
UNIVERSAL TIME

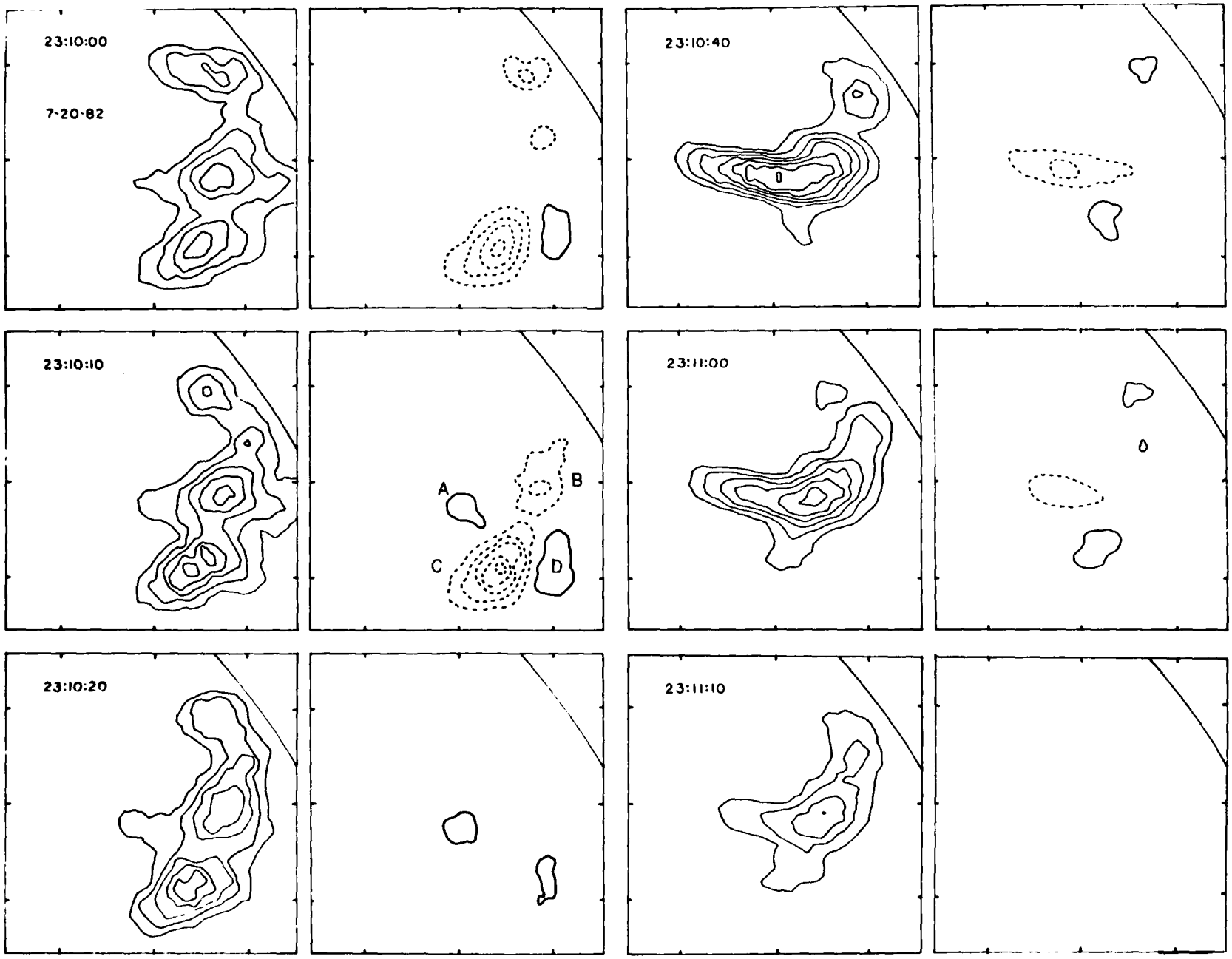
23:10:00
7-20-82
23:10:40
23:10:10
A
B
C
D
23:11:00
23:10:20
23:11:10


30
7-20-82
21:49:30


30
7-20-82
21:49:30


DA
FILM